# On the Spreading Resistance of Thin-Film Contacts

Peng Zhang, *Student Member, IEEE*, Y. Y. Lau, *Fellow, IEEE*, and Roland S. Timsit

***Abstract*—The spreading resistance of a microscopic area of contact (the "$a$-spot") located in a thin film is studied for both Cartesian and cylindrical geometries. The effect of film thickness $h$ on the spreading resistance is evaluated over a large range of aspect ratios. In the limit $h \to 0$, the normalized thin-film spreading resistance $\overline{R}_s$ converges to the finite values, i.e., 2.77 for the Cartesian case and 0.28 for the cylindrical case. An interpretation of these limits is given. Extension to a general $a$-spot geometry is proposed.**

***Index Terms*—Constriction resistance, contact resistance, electrical contacts, skin depth, spreading resistance, thin films.**

## I. Introduction

THIN-FILM contact is a very important issue in many areas, such as integrated circuits [1], thin-film devices [2], carbon nanotube and carbon nanofiber-based cathodes and interconnects [3], and microelectromechanical system [4], etc. Electrical contact has surfaced as a crucial problem in the ongoing studies at the University of Michigan of wire-array Z-pinch [5], high-power microwave generation [6] and protection [7], triple-point junctions [8], field emitters [9], and heating phenomenology [10].

Holm's classical $a$-spot model [11] gives the electrical spreading resistance of a circular constriction in a bulk interface of uniform resistivity as

$$R_s = \frac{\rho}{4a} \tag{1}$$

where $\rho$ and $a$ are the resistivity of the conductor and the radius of the constriction, respectively. The spreading resistance $R_s$ stems from the spreading of electrical field lines (current flow lines) from the constriction toward the bulk of the conductor. The contact resistance, or constriction resistance, between two bulk solids of same materials is $R_c = 2R_s = \rho/2a$. Equation (1) is the basis of many subsequent works [12]–[17]. Although recent generalizations of Holm's $a$-spot have included the effects of 3-D contact geometries [13], [14], [18], [19] and of dissimilar materials [20], [21], these generalizations are inapplicable to the thin-film contact, as shown in Fig. 1. This is because in a thin-film contact, spreading resistance arises from the sharp bending of current flow lines in the immediate vicinity of the constriction edges, with subsequent spreading into the thin film over a distance of one constriction radius or less [22]–[24]. Beyond this distance, the current flow lines are parallel to the film boundaries, and any additional contribution of spreading resistance to overall resistance becomes insignificant. In this paper, we focus on the spreading resistance in the thin film schematically illustrated in Figs. 1 and 2.

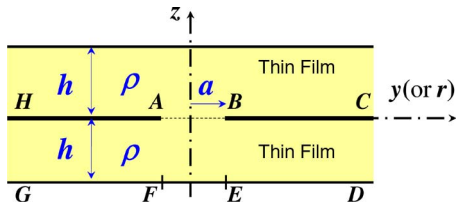


Fig. 1. Cylindrical (or Cartesian) electrical contact between two thin films of the same material. The $z$-axis is the axis of rotation for the cylindrical geometry.

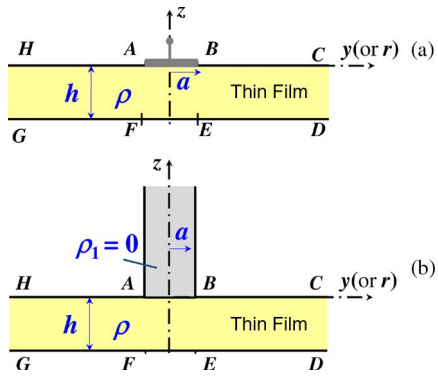


Fig. 2. Cylindrical or Cartesian geometries for the (a) electrode directly applied on the thin film and the (b) region of zero resistivity in contact with the thin film. The $z$-axis is the axis of rotation for the cylindrical geometry. For both (a) and (b), the boundary conditions, the potential profile, and therefore the spreading resistance in the thin film are equivalent to that in Fig. 1.

Referring to Fig. 1, due to symmetry, the $a$-spot area (the constriction interface AB) is an equipotential surface, and all current flow lines are perpendicular to this interface. This is also the situation for the two cases shown in Fig. 2, where Fig. 2(a) shows an electrode of size $a$ being applied directly to the conducting thin film, and Fig. 2(b) shows a post of zero resistivity kept in contact with the thin film with an interface of size $a$. Thus, the boundary conditions, the potential profile, and therefore the spreading resistance in the thin-film region are equivalent in all three geometries shown in Figs. 1 and 2, for both Cartesian and cylindrical geometries. Once we know the spreading (or constriction) resistance of any one case, the result will be immediately applicable to the other two cases.

By convention [21]–[24], the thin-film spreading resistance $R_s$ here is *defined* as

$$R_s = R_T - R_{\text{bulk}} \tag{2}$$

Manuscript received February 17, 2012; revised March 28, 2012; accepted April 6, 2012. Date of publication May 15, 2012; date of current version June 15, 2012. This work was supported in part by an Air Force Office of Scientific Research Grant on the Basic Physics of Distributed Plasma Discharges, by AFOSR Award FA9550-09-1-0662, L-3 Communications Electron Device Division, and Northrop Grumman Corporation. P. Zhang gratefully acknowledges a fellowship from the University of Michigan Institute for Plasma Science and Engineering. The review of this paper was arranged by Editor A. Schenk.

P. Zhang and Y. Y. Lau are with the Department of Nuclear Engineering and Radiological Sciences, University of Michigan, Ann Arbor, MI 48109 USA (e-mail: umpeng@umich.edu; yylau@umich.edu).

R. S. Timsit is with Timron Scientific Consulting, Inc., Toronto, ON M5M 1L6, Canada (e-mail: rtimsit@timron-inc.com).

Color versions of one or more of the figures in this paper are available online at http://ieeexplore.ieee.org.

Digital Object Identifier 10.1109/TED.2012.2195317

which is the difference between the total resistance, i.e., $R_T$, from AB to CD (and GH) and the bulk resistance, i.e., $R_{\rm bulk}$, from BE to CD and from AF to GH [cf. Fig. 2(a)]. The bulk resistances [21]–[24] are

$$R_{\rm bulk} = \rho(b-a)/2hW, \quad \text{[Cartesian]} \tag{3a}$$

$$R_{\rm bulk} = (\rho/2\pi h)\ell n(b/a), \quad \text{[cylindrical]} \tag{3b}$$

for the Cartesian case and cylindrical case, respectively, where $W$ in the Cartesian geometry denotes the channel width in the third ignorable dimension that is perpendicular to the paper, and $b$, which is not labeled in Figs. 1 and 2, is the $y$ (or $r$) coordinate of the boundary point C for the Cartesian (or cylindrical) case. All other symbols have been defined in Figs. 1 and 2. It is worth noting that our choice of the bulk resistance, i.e., $R_{\rm bulk}$ in (3), is *arbitrary* and, therefore, so is the definition of the spreading resistance $R_s$ in (2). This is because the current flow lines do not sharply curve and become parallel to the thin-film surface exactly at $y$ (or $r$) $= a$ (cf. Figs. 4 and 6). Despite the arbitrariness of the definitions of $R_s$ and $R_{\rm bulk}$, the total resistance $R_T = R_s + R_{\rm bulk}$, which is obtained directly from exact calculations and numerical simulations, remains the same. To be consistent with [21]–[24], we shall continue to use (2) and (3) as definitions of $R_s$ and $R_{\rm bulk}$ in this paper. As we shall see, this definition allows ready extension of the theory to a general $a$-spot geometry in the limit $h \to 0$ ($h =$ film thickness, cf. Fig. 1). We shall pay close attention to this limiting case in our interpretation of the results.

It is worth mentioning that the spreading resistance for the configuration shown in Fig. 2(a) was treated by other workers [25]–[30]. In these works, the boundary GD was an equipotential surface so that the current flow just above GD was *orthogonal* to GD. In contrast, in this paper, the current flow just above GD is *parallel* to GD, as we impose a constant potential on the boundaries CD and HG [22]–[24]. As a result, there is a key difference in the limit $h \to 0$, where the total resistance *vanishes* in [25]–[30] as the current path length vanishes, whereas in this paper, the total resistance becomes *infinite* because the cross-sectional area of current flow vanishes.

In Section II, we consider the dc Cartesian thin film. In Section III, we consider the dc cylindrical thin film. Concluding remarks are given in Section IV, where extensions of the model are suggested.

## II. Thin-Film Contact in Cartesian Geometry

The Cartesian thin-film geometry in Fig. 2(a) was studied by Hall [2] using conformal mapping calculation. If the spreading resistance is defined in (2) and (3a), Hall's exact calculation yields (cf. [2, Fig. 2] and [2, eq. (12)])

$$R_s = \frac{\rho}{4\pi W}\overline{R}_s \tag{4}$$

$$\overline{R}_s = 2\pi\frac{a}{h} - 4\ln\left[\sinh\left(\frac{\pi}{2}\frac{a}{h}\right)\right] \tag{5}$$

where $W$ denotes the channel width in the third ignorable dimension, and the rest of the symbols have been defined in Figs. 1 and 2.[1] The normalized thin-film spreading resistance, i.e., (5), is plotted in Fig. 3. Most recently, Zhang *et al.* [23] have analytically calculated the spreading (or contact) resistance of the Cartesian thin-film geometry in Fig. 2(b) by using the series expansion method (cf. [23, eq. (A8)] and [23, Fig. 5]. In the limit of $\rho_1 \to 0$ in Fig. 2(b) ($\rho_1 = 0.01\rho$ was used in [23]), their theory gives identical results to that of Hall, i.e., (5), as shown in Fig. 3.

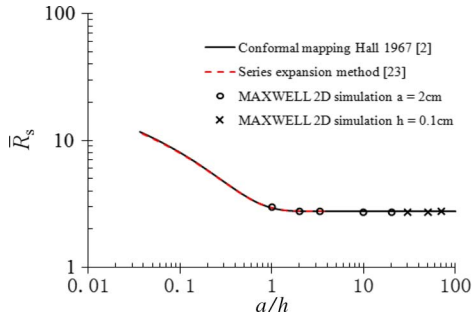


Fig. 3. Normalized thin-film spreading resistance $\overline{R}_s$ as a function of $a/h$, for the Cartesian structure in Figs. 1 and 2. The solid line is for the conformal mapping calculations [see eq. (5)]. The dashed line, which overlaps with the solid line, is for the series expansion calculations (cf. [23, eq. (A8)]). The symbols are for the MAXWELL 2-D simulation. Two sets of simulation were performed. The first set (circles) was fixed at $a = 2$ cm, and varying $h$ from 2 to 0.1 cm; the second set (crosses) was fixed at $h = 0.1$ cm, and varying $a$ from 3 to 7 cm.

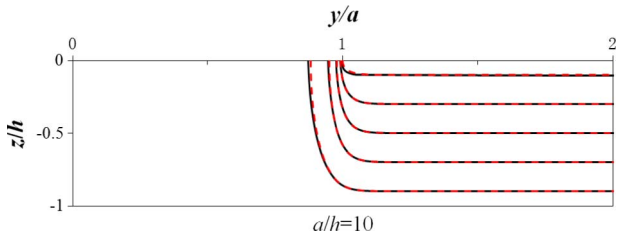


Fig. 4. Field lines in the right half of the Cartesian thin film in Figs. 1 and 2, calculated from both series expansion method (cf. [23, eq. (A8)]) (solid lines) and conformal mapping [2] (dashed lines), for the case of $a/h = 10.1$. In the series expansion method, we set $\rho_1 = 0.01\rho$ in Fig. 2(b).

It is easy to show from (5) that in the limit of $a/h \to \infty$, $\overline{R}_s$ converges to the constant minimum value of $4\ell n2 = 2.77$, which is valid for $a/h > 2$, as shown in Fig. 3. It is worth noting that the conformal mapping calculation is exact, without any approximation, and is therefore valid for arbitrary values of $a$ and $h$, even when $a$ and $h$ become arbitrarily small.[1] The field lines in the right half of the Cartesian thin film in Figs. 1 and 2 are shown in Fig. 4. These field lines were obtained by the series expansion method [23] on the model shown in Fig. 2(b). In addition, shown in Fig. 4 is the validation using the exact solution of conformal mapping [2].

To further confirm the *nonzero* limit of $\overline{R}_s = 2.77$ as $h \to 0$ for the Cartesian thin-film contact, we performed numerical simulations by using the MAXWELL 2-D code[2] for various combinations of parameters on the geometry shown in Fig. 2(a). The MAXWELL 2-D code results are included in Fig. 3.[1] The finite-element-method-based MAXWELL 2-D simulations were performed with great accuracy—the convergence iteration error was controlled to be $< 0.002\%$ for each case represented

[1]The $r$ (or $y$) coordinates of the boundary points C and H is $b$ (not shown in Figs. 1 and 2). We assume that $b \gg a$ or $b \gg h$, in which case all formulas in this paper are valid. See [23] for a detailed explanation. In all MAXWELL 2-D simulations shown in Figs. 3 and 5, we fixed $b = 8.8$ cm.

[2]See http://www.ansoft.com for MAXWELL 2-D software. For the present electrostatic problem, MAXWELL 2-D uses automatic meshing and finite-element analysis to solve the Laplace equation.

by the symbols in Fig. 3. It is clear that the simulations are in excellent agreement with the analytical calculations, from both conformal mapping [2] and series expansion method [23].

To further probe into the nonzero limit of $R_s = (4\ell n2) \times (\rho/4\pi W) \cong 2.77 \times (\rho/4\pi W)$ as $h \to 0$, at a finite value of $a$, let us compute the width $a'$ such that the bulk resistance between $y = a'$ and $y = b$ (and between $y = -a'$ and $y = -b$)[1] is equal to the total resistance $R_T$ as $h \to 0$. Thus, we have $R_T = \rho(b - a')/2Wh = R_s + R_{\rm bulk} = (4\ell n2) \times (\rho/4\pi W) + \rho(b - a)/2Wh$, yielding

$$a' = a\left(1 - \frac{2\ell n2}{\pi} h/a\right) = a(1 - 0.44h/a), \quad h/a \ll 1. \quad (6)$$

Thus, $a' = 0.956a$ if $h/a = 0.1$, as in Fig. 4. That is, the distance between $a'$ and $a$ gives the length scale over which the spreading resistance occurs (see Fig. 4). Note the possibility of enhanced local heating between $a'$ and $a$ because of the crowding of the field lines there. Such localized enhanced heating has been observed in bulk electrical contacts [31], but its contribution to contact overheating may be greatly magnified in a thin-film contact.

Another interpretation of $a'$ in the limit $h \to 0$ follows. We may express the total resistance as $R_T = R'_s + R'_{\rm bulk}$. Let $R'_{\rm bulk} = \rho(b - a')/2hW$. Then the residual resistance $R'_s = 0$ in the limit $h \to 0$. Comparing with (2), this shows the arbitrariness in the decomposition of the total thin-film resistance into the bulk and spreading resistance. It was the total resistance that Hall [2] calculated.

## III. Thin-Film Contact in Cylindrical Geometry

The $(r$–$z)$ geometry of a cylindrical thin film cannot be treated with conformal mapping. The spreading resistance of a thin conducting film for the cylindrical geometry (see Fig. 1) was analytically calculated by Timsit (cf. [24, Fig. 7] and [24, eq. (18)]), who approximated the current density distribution through the $a$-spot of this film with the known current density distribution through the $a$-spot in a semi-infinite bulk solid [14]. Timsit stated that this approximation is reliable only for $0 < a/h \leq 0.5$ [24] (cf. dashed curve in Fig. 5). Most recently, Zhang *et al.* [23] have confirmed Timsit's results for $0 < a/h \leq 0.5$ and extended his results for $a/h$ up to ten (cf. [23, Fig. 10]). Their results, obtained from the exact theory of series expansion, were synthesized into a simple useful polynomial[1] [23], as (7) and (8), shown at the bottom of the page, where the spreading resistance $R_s$ was defined in (2) and (3b). The solid curve in Fig. 5 plots (8), suggesting a finite constant value of about 0.28 for $\overline{R}_s$ as $a/h \to \infty$. Existence of a similar nonzero asymptotic limit was *proved* for the Cartesian case.

To verify the *nonzero* limit of $\overline{R}_s \cong 0.28$ as $h \to 0$ for the cylindrical thin-film contact, we performed the MAXWELL 2-D simulation[2] for various combinations of parameters on the geometry shown in Fig. 2(a). The MAXWELL 2-D code results are included in Fig. 5.[1] Similar to the Cartesian case, the simulations were performed with great accuracy—the convergence iteration error was controlled to be $< 0.002\%$ for each data point represented by symbols in Fig. 5. It is clear from Fig. 5 that the simulations are in excellent agreement with the analytical calculations and yield the asymptotic constant value of $\sim$0.28. The field lines in the right half of the thin film for the cylindrical geometry in Figs. 1 and 2 are shown in Fig. 6. Note the striking resemblance of the field lines in Figs. 4 and 6.

To further probe into the nonzero limit of $R_s \cong 0.28 \times (\rho/4a)$ as $h \to 0$ at a finite value of $a$, let us compute the radius $a'$ such that the bulk resistance between $r = a'$ and $r = b$ is equal to the total resistance $R_T$ as $h \to 0$. Thus, we have $R_T = (\rho/2\pi h)\ell n(b/a') = R_s + R_{\rm bulk} = 0.28 \times (\rho/4a) + (\rho/2\pi h)\ell n(b/a)$, yielding

$$a' = ae^{-0.28 \times \frac{\pi}{2}\frac{h}{a}} = ae^{\frac{-0.44h}{a}} \cong a(1 - 0.44h/a), \quad h/a \ll 1 \quad (9)$$

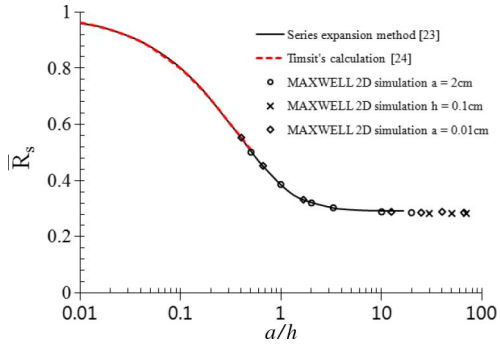


Fig. 5. Normalized thin-film spreading resistance $\overline{R}_s$ as a function of $a/h$, for the cylindrical structure in Figs. 1 and 2. The solid line is for (8), synthesized from the results of series expansion calculations (cf. [23, eq. (B8)]); the dashed line is for Timsit's calculations (cf. [24, eq. (18)]); and the symbols are for the MAXWELL 2-D simulation. Three sets of simulation were performed. The first set was fixed at $a = 2$ cm (circles), and varying $h$ from 2 to 0.1 cm; the second set was fixed at $h = 0.1$ cm (crosses), and varying $a$ from 3 to 7 cm; and the third set was fixed at $a = 0.01$ cm (diamonds), and varying $h$ from 0.025 to 0.00015 cm.

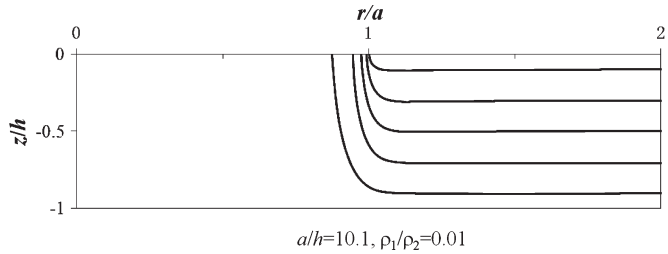


Fig. 6. Field lines in the right half of the cylindrical thin film in Fig. 2(b), calculated from the series expansion method (cf. [23, eq. (B8)]), for the case of $a/h = 10.1$ and $\rho_1 = 0.01\rho$.

$$R_s = \frac{\rho}{4a}\overline{R}_s \quad (7)$$

$$\overline{R}_s(a/h) = \begin{cases} 1 - 2.2968(a/h) + 4.9412(a/h)^2 - 6.1773(a/h)^3 + 3.811(a/h)^4 - 0.8836(a/h)^5, & 0.001 \leq a/h \leq 1 \\ 0.295 + 0.037(h/a) + 0.0595(h/a)^2, & 1 < a/h < 10 \end{cases} \quad (8)$$

which is identical to (6), derived for the Cartesian thin film. Thus, $a' = 0.956a$ if $h/a = 0.1$, as in Fig. 6 (and in Fig. 4). The distance between $a'$ and $a$ gives the length scale over which the spreading resistance occurs (see Fig. 6). The nonzero limit of $R_s \cong 0.28 \times (\rho/4a)$ as $h \to 0$, at a finite value of $a$, is equivalent to the resistance of a "residual" circular ring of thickness $h$ and of outer radius $a$ and inner radius $a'$

$$R_s = R_{\text{residual circular ring}} = \frac{\rho}{2\pi h}\ell n\left(\frac{a}{a'}\right) = \frac{\rho}{2\pi h}\ell n\left(\frac{1}{1-0.44h/a}\right) \cong 0.28 \times \frac{\rho}{4a}, \quad h \to 0 \quad (10)$$

where (3b) and (9) have been used. As seen from (10), as $h$ decreases to zero, the resistance of the "residual" circular ring region (over which the spreading resistance occurs) remains a constant, and this might be considered as an interpretation of the *nonzero* limit of the spreading resistance $R_s \cong 0.28 \times (\rho/4a)$ as $h \to 0$ for the cylindrical case.

A similar argument may be made for the Cartesian case as (9) and (6) are identical. The distance between $a$ and $a'$ remains to be $0.44h$, and (10) is modified to read [cf. eq. (3a)]

$$R_s = R_{\text{residual rectangular strips}} = \frac{\rho(a-a')}{2hW} = \frac{\rho \times 0.44h}{2hW} = \frac{\rho}{4\pi W} \times 2.77, \quad h \to 0. \quad (11)$$

Once $a$ is fixed, in the limit $h \to 0$, the edge "B" in Fig. 2(a) looks the same whether it is a circular arc (cylindrical geometry) or a straight line segment pointing out of the paper (Cartesian geometry), as far as the current flow patterns at B are concerned. This is why the factor 0.44 appears in both (6) and (9), and Figs. 4 and 6 look identical. Since $0.28 = (4\ell n2)/\pi^2$, we conjecture that the asymptotic value for the cylindrical thin-film spreading resistance is $\overline{R}_s = (4\ell n2)/\pi^2 = 2.77/\pi^2 = 0.28$ as $h \to 0$. The ratio between the "hard limits" of $\overline{R}_s$ for the Cartesian and cylindrical thin film is $\pi^2$ as $h \to 0$.

Finally, although $R_s$ approaches a finite constant as $h \to 0$, $R_s/R_T$ approaches to zero since $R_{\text{bulk}}$, and therefore, $R_T$ approaches infinity [cf. eq. (3)]. That is, the spreading resistance contributes to a negligible fraction of the total resistance in the limit $h \to 0$. The latter property was also shared in [25]–[30], although in these references, both the total resistance and the spreading resistance vanish as $h \to 0$.

## IV. Concluding Remarks

In this paper, we study the spreading resistance in the thin-film contact shown in Figs. 1 and 2, for both Cartesian and cylindrical geometries. The calculations were performed by three very different methods: conformal mapping [2], [22], [23], infinite series expansion [23], and Maxwell 2-D code[2], all yielding the same results. Most importantly, we found that the normalized thin-film spreading resistance $\overline{R}_s$ converges to the finite values, i.e., 2.77 for Cartesian and 0.28 for the cylindrical case in the limit $h \to 0$. An interpretation of these asymptotic limits in terms of the residual resistance between $a'$ and $a$ is given [see eqs. (10) and (11)]. The crowding of the field lines between $a$ and $a'$ could lead to significant ohmic heating there (see Figs. 4 and 6).

Current crowding is a well-known phenomenon in the area of contact resistance, for example in metal–semiconductor contacts where current crowding may have a significant effect on contact resistance [32]. We point out that there are differences between metal–metal and metal–semiconductor contacts. For example, in the transmission line model of a metal–semiconductor contact [32], [33], the length scale over which most of the current from a contact into a semiconductor thin film flows is called the transfer length, $L_T$. From (6) and Fig. 4, one may argue that $L_T \sim 0.44h$ for the present Cartesian thin-film model, and this transfer length is due only to the fringing fields. In the transmission line model [32], there is another component of transfer length, neglecting the fringing fields, that is approximately given by $L_{T2} = (r_c/r_s)^{1/2}$, where $r_s = \rho/h$ is the sheet resistance (in $\Omega$/square) in the semiconductor thin film under the contact, and $r_c = A_c\rho_c$, where $A_c =$ contact area, and $\rho_c =$ contact resistivity. The resistivity $\rho_c$ arises from the metal–semiconductor barrier so that this paper would have $\rho_c = 0$, yielding $L_{T2} = 0$ in the conventional transmission line model [32]. The transmission line model does not include the effect of fringing fields studied in this paper.

Since the distance between $a$ and $a'$ is *always* $0.44h$ as $h \to 0$ [cf. eqs. (6) and (9)], and Figs. 4 and 6 are identical for both cylindrical and Cartesian $a$-spot shown in Fig. 1, we might extend the theory to an $a$-spot of an arbitrary shape in the $h \to 0$ limit. We propose that for the model shown in Fig. 2(a) in particular, the spreading resistance $R_s$ defined in (2) would assume the general form

$$R_s = \left(\frac{\rho}{L}\right)\frac{2\ell n2}{\pi}, \quad h \to 0 \quad (12)$$

where $L$ is the circumference of the $a$-spot of an arbitrary shape, and $R_{\text{bulk}}$ is the bulk resistance of the thin film exterior to this generalized $a$-spot. For a circular $a$-spot of radius $a$, $L = 2\pi a$, and (12) reproduces (10). For an $a$-spot in the Cartesian geometry, $L = 2W$ [the factor of two to account for both edges A and B in Fig. 2(a)], and (12) reproduces (11). Clearly, there will be limitations to the validity of (12), particularly if the $a$-spot shape is highly irregular, e.g., where the radius of curvature $s$ of the $a$-spot significantly varies in magnitude and sign along the circumference. For $a$-spots that do not deviate too strongly from circular or rectangular geometry, and from our comments following (11), (12) is expected to be valid if $h \ll$ minimum $s$.

Finally, Timsit pointed out that the dc spreading resistance in a thin film is comparable to the spreading resistance for high-frequency ac current in a bulk solid where the current flow is limited to the skin depth [24], if the thickness of the equivalent thin film is identified as the skin depth at the relevant frequency, i.e., $h = \delta$. Along this line, we speculate that the same finite limits of $\overline{R}_s = 2.77$ for the Cartesian case and $\overline{R}_s = 0.28$ for the cylindrical case would apply to the ac case as the skin depth $\delta \to 0$. In fact, Fig. 9 of [24] for the 1-GHz curve is about 0.3 of that for the cylindrical dc curve, for all constriction diameters shown in that figure. If the frequency further increases, we expect the ratio would be $\sim$0.28. Likewise, we conjecture that Fig. 10 of [24] would converge to the final value of $\sim$0.28 as $a/\delta \to \infty$. If our conjecture is correct, the limiting value of spreading resistance would give rise to an important component of contact resistance at high signal frequencies.

## REFERENCES


[1] W. J. Greig, *Integrated Circuit Packaging, Assembly and Interconnections*. New York: Springer-Verlag, 2007.

[2] P. M. Hall, "Resistance calculations for thin film patterns," *Thin Solid Films*, vol. 1, no. 4, pp. 277–295, Jan. 1968.

[3] R. H. Baughman, A. A. Zakhidov, and W. A. de Heer, "Carbon nanotubes—The route toward applications," *Science*, vol. 297, no. 5582, pp. 787–792, Aug. 2002.

[4] M. B. Read, J. H. Lang, A. H. Slocum, and R. Martens, "Contact resistance in flat thin films," in *Proc. 55th IEEE Holm Conf. Elect. Contacts*, 2009, pp. 303–309.

[5] M. R. Gomez, J. C. Zier, R. M. Gilgenbach, D. M. French, W. Tang, and Y. Y. Lau, "Effect of soft metal gasket contacts on contact resistance, energy deposition, and plasma expansion profile in a wire array Z pinch," *Rev. Sci. Instrum.*, vol. 79, no. 9, p. 093512, Sep. 2008.

[6] R. M. Gilgenbach, Y. Y. Lau, H. McDowell, K. L. Cartwright, and T. A. Spencer, "Crossed-field devices," in *Modern Microwave and Millimeter Wave Power Electronics*, R. J. Barker, N. C. Luhmann, J. H. Booske, and G. S. Nusinovich, Eds. Piscataway, NJ: IEEE Press, 2004, ch. 6.

[7] P. Zhang, Y. Y. Lau, M. Franzi, and R. M. Gilgenbach, "Multipactor susceptibility on a dielectric with a bias dc electric field and a background gas," *Phys. Plasmas*, vol. 18, no. 5, pp. 053508-1–053508-8, May 2011.

[8] N. M. Jordan, Y. Y. Lau, D. M. French, R. M. Gilgenbach, and P. Pengvanich, "Electric field and electron orbits near a triple point," *J. Appl. Phys.*, vol. 102, no. 3, pp. 033301-1–033301-10, Aug. 2007.

[9] R. Miller, Y. Y. Lau, and J. H. Booske, "Electric field distribution on knife-edge field emitters," *Appl. Phys. Lett.*, vol. 91, no. 7, pp. 074105-1–074105-3, Aug. 2007.

[10] P. Zhang, Y. Y. Lau, and R. M. Gilgenbach, "Analysis of radio-frequency absorption and electric and magnetic field enhancements due to surface roughness," *J. Appl. Phys.*, vol. 105, no. 11, pp. 114908-1–114908-9, Jun. 2009.

[11] R. Holm, *Electric Contact*, 4th ed. Berlin, Germany: Springer-Verlag, 1967.

[12] R. S. Timsit, "Electrical contact resistance: Fundamental principles," in *Electrical Contacts: Principles and Applications*, P. G. Slade, Ed. New York: Marcel Dekker, 1999, p. 1.

[13] A. M. Rosenfeld and R. S. Timsit, "The potential distribution in a constricted cylinder: An exact solution," *Quart Appl. Math.*, vol. 39, pp. 405–417, Oct. 1981.

[14] R. S. Timsit, "Electrical contact resistance: Properties of stationary interfaces," *IEEE Trans. Compon. Packag. Technol.*, vol. 22, no. 1, pp. 85–98, Mar. 1999.

[15] M. Nakamura, "Constriction resistance of conducting spots by the boundary element method," *IEEE Trans. Compon., Hybrids, Manuf. Technol.*, vol. 16, no. 3, pp. 339–343, May 1993.

[16] Y. H. Jang, J. R. Barber, and S. J. Hu, "Electrical conductance between conductors with dissimilar temperature-dependent material properties," *J. Phys. D, Appl. Phys.*, vol. 31, no. 22, p. 3197, Nov. 1998.

[17] J. L. Carbonero, G. Morin, and B. Cabon, "Comparison between beryllium-copper and tungsten high frequency air coplanar probes," *IEEE Trans. Microw. Theory Tech.*, vol. 43, no. 12, pp. 2786–2793, Dec. 1995.

[18] Y. Y. Lau and W. Tang, "A higher dimensional theory of electrical contact resistance," *J. Appl. Phys.*, vol. 105, no. 12, pp. 124902-1–124902-10, Jun. 2009.

[19] M. R. Gomez, D. M. French, W. Tang, P. Zhang, Y. Y. Lau, and R. M. Gilgenbach, "Experimental validation of a higher dimensional theory of electrical contact resistance," *Appl. Phys. Lett.*, vol. 95, no. 7, pp. 072103-1–072103-3, Aug. 2009.

[20] P. Zhang and Y. Y. Lau, "Scaling laws for electrical contact resistance with dissimilar materials," *J. Appl. Phys.*, vol. 108, no. 4, pp. 044914-1–044914-9, Aug. 2010.

[21] P. Zhang, Y. Y. Lau, W. Tang, M. R. Gomez, D. M. French, J. C. Zier, and R. M. Gilgenbach, "Contact resistance with dissimilar materials: bulk contacts and thin film contacts," presented at the Proc. 57th IEEE Holm Conf. Electrical Contacts, Minneapolis, MN, 2011, Paper 2.2.

[22] P. Zhang, Y. Y. Lau, and R. M. Gilgenbach, "Minimization of thin film contact resistance," *Appl. Phys. Lett.*, vol. 97, no. 20, pp. 204103-1–204103-3, Nov. 2010.

[23] P. Zhang, Y. Y. Lau, and R. M. Gilgenbach, "Thin film contact resistance with dissimilar materials," *J. Appl. Phys.*, vol. 109, no. 12, pp. 124910-1–124910-10, Jun. 2011.

[24] R. S. Timsit, "Constriction resistance of thin-film contacts," *IEEE Trans. Compon. Packag. Technol.*, vol. 33, no. 3, pp. 636–642, Sep. 2010.

[25] S. Kristiansson, F. Ingvarson, and K. O. Jeppson, "Compact spreading resistance model for rectangular contacts on uniform and epitaxial substrates," *IEEE Trans. Electron Devices*, vol. 54, no. 9, pp. 2531–2536, Sep. 2007.

[26] A. Nussbaum, "Capacitance and spreading resistance of a stripe line," *Solid State Electron.*, vol. 38, no. 6, pp. 1253–1256, Jun. 1995.

[27] M. S. Leong, S. C. Choo, and L. S. Tan, "The role of source boundary condition in spreading resistance calculations," *Solid State Electron.*, vol. 21, no. 7, pp. 933–941, Jul. 1978.

[28] R. H. Cox and H. Strack, "Ohmic contacts for GaAs devices," *Solid State Electron.*, vol. 10, no. 12, pp. 1213–1218, Dec. 1967.

[29] B. Gelmont and M. Shur, "Spreading resistance of a round ohmic contact," *Solid State Electron.*, vol. 36, no. 2, pp. 143–146, Feb. 1993.

[30] M. W. Denhoff, "An accurate calculation of spreading Resistance," *J. Phys. D, Appl. Phys.*, vol. 39, no. 9, pp. 1761–1765, May 2006.

[31] J. A. Greenwood and J. B. P. Williamson, "Electrical conduction in solids. II. Theory of temperature-dependent conductors," *Proc. R. Soc. A*, vol. 246, no. 1244, pp. 13–31, Jul. 1958.

[32] D. K. Schroder, *Semiconductor Material and Device Characterization*., 2nd ed. New York: Wiley, 1998, p. 149.

[33] H. H. Berger, "Models for contacts to planar devices," *Solid State Electron.*, vol. 15, pp. 145–158, 1972.


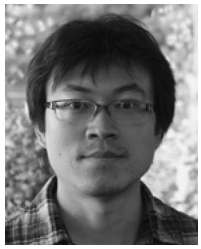

**Peng Zhang** (S'07) is a graduate student in Nuclear Engineering and Radiological Sciences at the University of Michigan. He has 12 refereed publications in surface sciences and plasmas. He received the IEEE Nuclear and Plasma Sciences Graduate Scholarship Award.

**Y. Y. Lau** (M'98–SM'06–F'08) received all degrees (SB-SM-PhD) in EE from MIT. He is currently Professor at the University of Michigan, specialized in RF sources, heating, and discharge. A Fellow of IEEE and of American Physical Society, he received the IEEE Plasma Science and Applications Award.

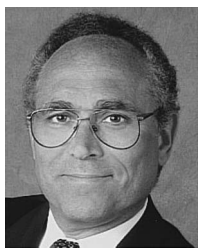

**Roland S. Timsit** received the Ph.D degree in physics in 1970 at the University of Toronto. He was Chief Technologist at Tyco Electronics. He received the IEEE Ragnar Holm Scientific Award and four international awards relating to electrical contacts. He is currently President of Timron Scientific Consulting Inc., an electronic connector design company.